JPEDAV (2016) 37:269–276
DOI: 10.1007/s11669-016-0453-3
1547-7037 ©ASM International

Interdiffusion and Atomic Mobility Studies in Ni-Rich fcc Ni-Co-Al Alloys

Y.L. Yang, Z. Shi, Y.S. Luo, Y. Lu, S.Y. Yang, J.J. Han, W.B. Li, C.P. Wang, and X.J. Liu

(Submitted October 2, 2015; in revised form January 12, 2016; published online February 17, 2016)

The ternary interdiffusion coefficients in fcc Ni-Co-Al alloys at 1373 K were determined using Whittle and Green method together with electronic-probe microanalysis. With the help of DICTRA software, the experimental diffusion coefficients were critically assessed to obtain the atomic mobilities of Ni, Co and Al in fcc Ni-Co-Al alloys. Comprehensive comparisons between calculated and experimental diffusion coefficients showed that the experimental data could be well reproduced by the atomic mobilities obtained in the present work. The developed diffusion mobilities were further validated by the calculation of the concentration profiles and diffusion paths in diffusion couples.

Keywords atomic mobility, DICTRA, diffusion couple, interdiffusion coefficients, Whittle and Green method

1. Introduction

The nickel-base superalloys are high-temperature materials which display excellent resistance to mechanical and chemical degradation at temperature close to their melting points.[1] They were widely used to manufacture the blades of aircraft engine and steam turbine in the aerospace and many other industries.[2] The nickel-aluminum system is the most basic binary system for superalloys. As the content of aluminum added to γ phase increases, a secondary precipitation phase forms, thus the γ′ phase. This phase has an ordered intermetallic $L1_2$ crystal structure,[3] which is of great importance for its precipitation strengthening effect in the nickel-base superalloys. Cobalt is a γ partition element, which mainly forms the γ matrix phase in the nickel-base superalloys. In addition, cobalt can effectively reduce the stacking fault energy, and has a significant influence on creep-rupture behavior at elevated temperature[4] and coarsening rate of the γ′ phase.[5] Although many studies on ternary diffusion have been performed in the fcc solid solutions, such as Ni-Co-X (X = Re and Ru),[6,7] Ni-Co-Cr,[8]Ni-Al-Mn[9] and Ni-Al-X (X: Re, W),[10,11] the study on the Ni-Co-Al system is still missing. Due to the important effect of Al and Co on the formation, creep resistance and coarsening of the γ′ phase in nickel-based superalloys, it is essential to understand the diffusion behavior in the Ni-Co-Al system.

Thermodynamic calculation and kinetic simulation have become important to study material preparation and processes. DICTRA[12,13] is a powerful software for simulation of diffusion controlled transformations in multicomponent alloys. Combining the atomic mobility databases and the thermodynamic databases, DICTRA has thus been applied to investigate many different types of materials using different models. The key issue in various kinetics calculations in DICTRA is the foundation of atomic mobility databases. Therefore, the assessment of the atomic mobilities in nickel-base superalloys is extremely important.

As one of the key ternary system in the multicomponent nickel-based superalloys, Ni-Co-Al system was chosen as the target in the present work. The major purposes of the present work are: (1) to experimentally measure the interdiffusivities of fcc Ni-Co-Al alloys at 1373 K; (2) to review thermodynamic parameters and binary Ni-Co, Ni-Al and Co-Al atomic mobilities from literatures; (3) to assess the atomic mobilities of Ni-Co-Al system based on the critically reviewed literature as well as the present experimental results; (4) to verify the reliability of the presently obtained mobility parameters by comparing the calculated diffusivities, concentration profiles, and diffusion paths with the corresponding experimental data.

2. Experimental Procedures

Ni (purity: 99.95 wt.%), Co (purity: 99.9 wt.%) and Al (purity: 99.99 wt.%) were used as starting materials. Six diffusion couples, as shown in Table 1, were prepared in the following steps:

Firstly, terminal Ni-Al, Ni-Co, pure Ni and fcc Ni-Co-Al alloys with different compositions were melted using arc melting and casted into the buttons under an argon atmosphere. The buttons were re-melted five times to ensure homogeneities. The weight losses of alloys were all less than 1 wt.% during arc-melting.

Y.L. Yang, Z. Shi, Y.S. Luo, Y. Lu, S.Y. Yang, J.J. Han, C.P. Wang, and **X.J. Liu**, Department of Materials Science and Engineering, Fujian Key Laboratory of Materials Genome, College of Materials, Xiamen University, Xiamen 361005, People's Republic of China; **and W. B. Li,** Department of Aeronautics, Xiamen University, Xiamen 361005, People's Republic of China. Contact e-mail: shizhan@xmu.edu.cn.

Table 1 List of nine compositions of the six diffusion couples in the present work

Couple name	Composition (at.%)	Temperature, K	Diffusion time, s
A1	Ni/Ni-10.7Al-10.4Co	1373	259,200
A2	Ni/Ni-5.4Al-15.5Co	1373	259,200
B1	Ni-5.2Al/Ni-10.5Co	1373	259,200
B2	Ni-10.5Al/Ni-10.5Co	1373	259,200
B3	Ni-10.5Al/Ni-15.5Co	1373	259,200
B4	Ni-10.2Al/Ni-20.3Co	1373	259,200

Secondly, the buttons were cut into suitably sized blocks of $4\times4\times9$ mm^3 via wire-electrode discharging machining after mechanically polishing the surface. Then, it were sealed into an evacuated quartz tube, homogenized in an diffusion furnace at 1473 K for 2 days. After that, all the samples were grounded on SiC grind papers to remove surface contamination. The diffusion surface of each sample was polished with diamond paste to a finish of 0.25 μm.

Subsequently, diffusion couples were prepared by binding the polished surfaces of two samples together with Mo wire. Then the diffusion couples were sealed into evacuated quartz tubes, along with a small amount of titanium sponge to act as an oxygen getter. Annealing was carried out at 1373 K for 3 days, followed by ice water quenching. After that, the annealed couples were cut parallel to diffusion direction and then polished metallographically. Concentration profiles in these diffusion couples were measured by electronic-probe microanalysis (EPMA, JXA-8100, JEOL,Japan,the accelerating voltage and probe current were 20 kV, 1.0×10^{-8} A, respectively).

3. Evaluation and Modeling of Ternary Diffusivities

3.1 Evaluation of Ternary Diffusion Coefficients

According to Kirkaldy,[14] in a ternary alloy, Fick's second law of diffusion for a component i of concentration C_i in a ternary system can be given as

$$\frac{\partial C_i}{\partial t}=\sum_{j=1}^{2}\frac{\partial}{\partial x}\left(\tilde{D}_{ij}^{3}\frac{\partial C_j}{\partial x}\right)\quad \text{for } i=1,\ 2 \tag{Eq 1}$$

where x is the distance, t represents time, C_i is concentration of element i, and $\tilde{D}_{ij}^{3}$ are the interdiffusivities in which component 3 represents the solvent. The main interdiffusion coefficients, $\tilde{D}_{11}^{3}$ and $\tilde{D}_{22}^{3}$, represent the influence of the concentration gradients of elements 1 and 2 on their own fluxes. While $\tilde{D}_{12}^{3}$ and $\tilde{D}_{21}^{3}$ are the cross interdiffusion coefficients which represent the influences of the concentration gradients of element 2 and element 1 on the fluxes of each other. According to Prof. Morral,[15] all diffusivities have their hidden concentration unit, in present work, the concentration unit is moles of i/m^{3,} and the diffusivities is Molar density diffusivity, assuming constant molar volume.

Under the usual initial and boundary conditions prevalent for semi-infinite diffusion couples, we have

$$\begin{aligned} C_i(-x,0)&=C_i(-\infty,t)=C_i^{-}\\ C_i(x,0)\quad&=C_i(+\infty,t)=C_i^{+}\quad \text{for } i=1,\ 2\end{aligned} \tag{Eq 2}$$

Then the solutions of Eq 1 are

$$\int_{C_i^{-}}^{C_i} x\,dC_i=-2t\sum_{j=1}^{2}\tilde{D}_{ij}^{3}\frac{dC_j}{dx} \tag{Eq 3}$$

To avoid the calculating of Matano interface, Whittle and Green[16] introduce the normalized concentration parameter $Y_i=(C_i-C_i^{-})/(C_i^{+}-C_i^{-})$, then the Eq 3 can be transformed to

$$\frac{1}{2t}\frac{dx}{dY_1}\left[(1-Y_1)\int_{-\infty}^{x}Y_1\cdot dx+Y_1\int_{x}^{+\infty}(1-Y_1)\cdot dx\right]=\tilde{D}_{11}^{3}+\tilde{D}_{12}^{3}\frac{C_2^{+}-C_2^{-}}{C_1^{+}-C_1^{-}}\cdot\frac{dY_2}{dY_1} \tag{Eq 4}$$

$$\frac{1}{2t}\frac{dx}{dY_2}\left[(1-Y_2)\int_{-\infty}^{x}Y_2\cdot dx+Y_2\int_{x}^{+\infty}(1-Y_2)\cdot dx\right]=\tilde{D}_{22}^{3}+\tilde{D}_{21}^{3}\frac{C_1^{+}-C_1^{-}}{C_2^{+}-C_2^{-}}\cdot\frac{dY_1}{dY_2} \tag{Eq 5}$$

To solve for the four diffusion coefficients in Eq 4 and 5, two diffusion couples are required whose diffusion paths cross at a common concentration.

3.2 Modeling of Atomic Mobility

From absolute-reaction rate theory,[17,18] the mobility coefficient for an element B, M_B, may be divided into a frequency factor M_B^0 and an activation enthalpy Q_B,[19,20]

$$M_B=M_B^0\exp\left(-\frac{Q_B}{RT}\right)\frac{1}{RT}{}^{mg}\Gamma \tag{Eq 6}$$

where R is the gas constant and T is the absolute temperature, ${}^{mg}\Gamma$ is a factor taking into account the effect of the ferromagnetic transition,[21]which is a function of the alloy composition. It has been suggested[22] that one should expand the logarithm of the frequency factor, ln M_B^0 rather than the value itself, thus the mobility, M_B is expressed as:

$$M_B = \exp\left(\frac{RT\ln M_B^0}{RT}\right)\exp\left(-\frac{Q_B}{RT}\right)\frac{1}{RT}^{mg}\Gamma \qquad \text{(Eq 7)}$$

For the fcc phase, the ferromagnetic contribution to diffusion is negligible,[23] then M_B^0 and Q_B can be merged into one parameter:$\Phi_B = RT\ln M_B^0 - Q_B$, Φ_B can be represented by the Redlich–Kister polynomial[24] for binary terms and a power series expansion[25] for ternary terms:

$$\Phi_B = \sum_i x_i\Phi_B^i + \sum_i\sum_{j>i} x_ix_j\left[\sum_{r=0}^{m} {}^r\Phi_B^{i,j}\left(x_i - x_j\right)^r\right] + \sum_i\sum_{j>i}\sum_{k>j} x_ix_jx_k\left[v_{ijk}^s\,{}^s\Phi_B^{i,j,k}\right] \quad (s = i,\ j \text{ or } k) \qquad \text{(Eq 8)}$$

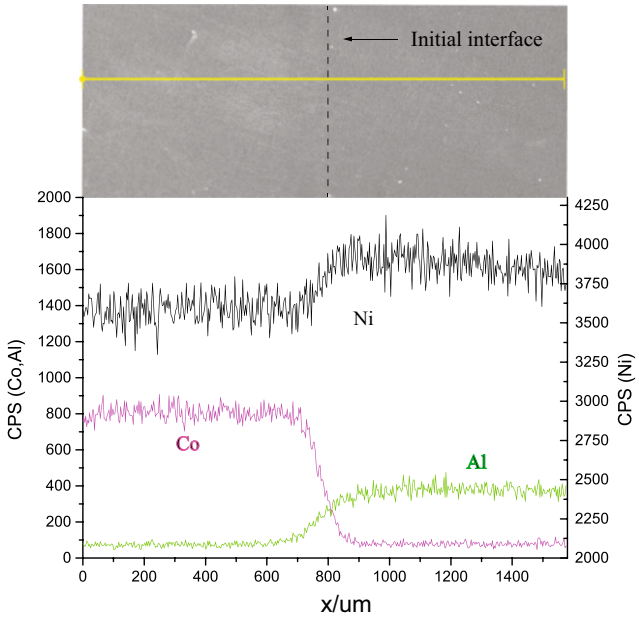

Fig. 1 The typical micrograph and rough concentration gradient of Couple B3 after annealing at 1373 K for 259,200 s

where x_i is mole fraction of element i, Φ_B^i is the value of Φ_B for pure i and thus represents one of the endpoint value in the composition space, ${}^r\Phi_B^{i,j}$ and ${}^s\Phi_B^{i,j,k}$ represent binary and ternary interaction parameters. For the parameter v_{ijk}^s, it can be expressed as

$$v_{ijk}^s = x_s + (1 - x_i - x_j - x_k)/3 \qquad \text{(Eq 9)}$$

where x_i, x_j, x_k and x_s are the mole fractions, i, j, k represent the three elements and $s = i$, j, or k.

The diffusion mobility can be related to the diffusion coefficient, assuming a mono-vacancy mechanism coupled neglecting correlation factors,[22] the tracer diffusivity D_{B}^* is directly related to the mobility M_{B} by means of the Einstein relation

$$D_{\mathrm{B}}^* = RTM_{\mathrm{B}} \qquad \text{(Eq 10)}$$

The interdiffusion coefficients with n as the dependent species are correlated to the atomic mobility by[20]

$$\tilde{D}_{kj}^n = \sum_i (\delta_{ik} - x_k)\cdot x_i \cdot M_i \cdot \left(\frac{\partial\mu_i}{\partial x_j} - \frac{\partial\mu_i}{\partial x_n}\right) \qquad \text{(Eq 11)}$$

where the Kronecker delta $\delta_{ik} = 1$ when $i = k$, otherwise $\delta_{ik} = 0$. The x_i,μ_i and M_i are the mole fraction, chemical potential and mobility of element i, respectively.

4. Result and Discussion

4.1 Interdiffusion Coefficients

Since all the diffusion took place in single fcc phase, typically micrograph were provide, as shown in Fig. 1, from which we can see the rough concentration gradient of all elements. Four interdiffusion coefficients $\tilde{D}_{AlAl}^{Ni}$, $\tilde{D}_{AlCo}^{Ni}$, $\tilde{D}_{CoCo}^{Ni}$, $\tilde{D}_{CoAl}^{Ni}$ are determined at the intersection composition of the diffusion paths based on the Whittle and Green method, using Eq 4 and 5. Table 2 presents the measured ternary main interdiffusion coefficients and the corresponding cross interdiffusion coefficients. The main interdiffusion coefficients are all positive, while the cross interdiffusion coefficients are positive or negative. The value of $\tilde{D}_{AlAl}^{Ni}$ is an

Table 2 Diffusion coefficients in fcc Ni-Co-Al alloys in the present work

Intersection diffusion paths	Composition (at.%)		Diffusion coefficients (10^{-15} m^2 s^{-1})			
	Co	Al	$\tilde{D}_{\mathrm{CoCo}}^{\mathrm{Ni}}$	$\tilde{D}_{\mathrm{CoAl}}^{\mathrm{Ni}}$	$\tilde{D}_{\mathrm{AlAl}}^{\mathrm{Ni}}$	$\tilde{D}_{\mathrm{AlCo}}^{\mathrm{Ni}}$
A1-B1	1.28	3.45	5.863	−0.350	22.476	-0.310
A1-B2	4.62	5.66	4.812	1.465	21.689	2.853
A1-B3	5.83	6.00	4.893	2.021	21.846	3.580
A1-B4	7.50	6.35	5.011	1.413	22.977	3.822
A2-B1	3.95	2.52	3.992	−4.083	20.899	−0.473
A2-B2	9.12	3.14	3.807	−2.434	12.693	0.727
A2-B3	11.7	3.59	3.347	0.472	13.682	0.565
A2-B4	14.7	3.76	2.428	−4.027	12.397	0.867

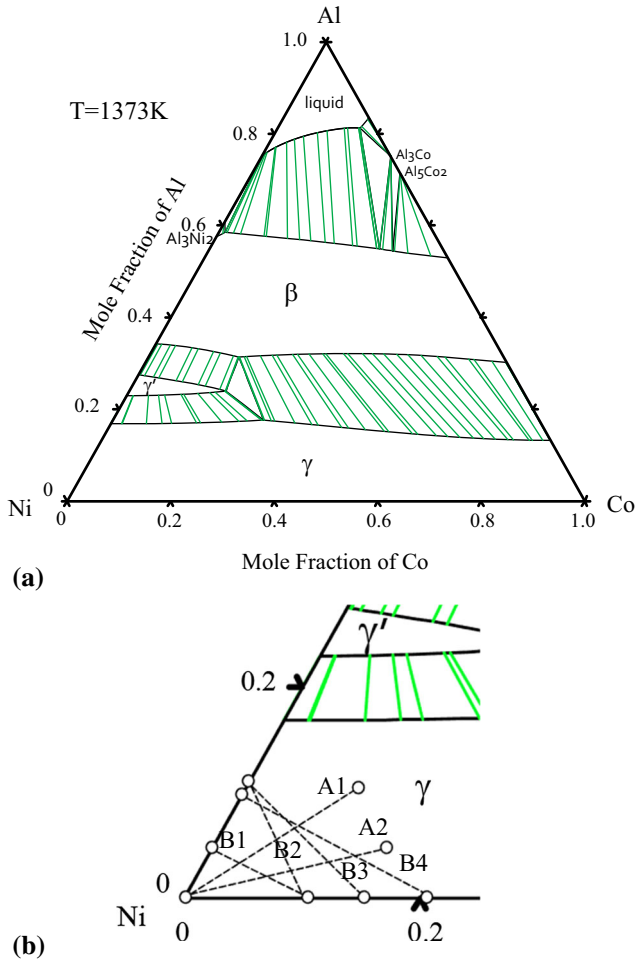

Fig. 2 (a) Calculated isothermal section at 1373 K in the Ni-Co-Al system using the thermodynamic parameters of Zhu et al.[27] (b) The six diffusion couples were shown in the Ni-rich area

order of magnitude higher than $\tilde{D}^{Ni}_{CoCo}$, indicating Al diffuse faster than Co, which can be seen from the concentration profile in Fig. 1 as well. All the presently obtained interdiffusion coefficients are further validated by the following constraints,[26]

$$\tilde{D}^{Ni}_{AlAl} + \tilde{D}^{Ni}_{CoCo} > 0 \qquad \text{(Eq 12)}$$

$$\tilde{D}^{Ni}_{AlAl} \cdot \tilde{D}^{Ni}_{CoCo} - \tilde{D}^{Ni}_{AlCo} \cdot \tilde{D}^{Ni}_{CoAl} \geq 0 \qquad \text{(Eq 13)}$$

$$\left(\tilde{D}^{Ni}_{AlAl} - \tilde{D}^{Ni}_{CoCo}\right)^2 + 4\tilde{D}^{Ni}_{AlCo} \cdot \tilde{D}^{Ni}_{CoAl} \geq 0 \qquad \text{(Eq 14)}$$

Substituting the presently obtained interdiffusion coefficients into Eq 12-14, it is found that they fulfilled these constraints. Therefore, the presently obtained interdiffusivities are considered to be reasonable.

Table 3 Assessed mobility parameters for the fcc Ni-Co-Al alloys (all in SI units)

Mobility	Parameter	Reference
Ni	$Q^{Ni}_{Ni} = -271{,}377.6 - 81.79T$	27
	$Q^{Al}_{Ni} = -144{,}600 - 64.85T$	27
	$Q^{Al,Ni}_{Ni} = -29{,}571.8$	27
	$Q^{Co}_{Ni} = -270{,}348 - 87.3T$	29
	$Q^{Co,Ni}_{Ni} = 7866 + 7.65T$	29
	$Q^{Co,Al}_{Ni} = 621{,}035.4$	This work
Co	$Q^{Co}_{Co} = -286{,}175 - 76.0T$	29
	$Q^{Ni}_{Co} = -284{,}169 - 67.6T$	29
	$Q^{Co,Ni}_{Co} = 10{,}787 - 11.5T$	29
	$Q^{Al}_{Co} = -172{,}082 - 28.422T$	28
	$Q^{Co,Al}_{Co} = -427{,}920$	28
	$Q^{Al,Ni}_{Co} = -170{,}373.3$	This work
Al	$Q^{Al}_{Al} = -123{,}111.6 - 97.34T$	27
	$Q^{Ni}_{Al} = -268{,}381\text{-}71.04T$	27
	$Q^{Al,Ni}_{Al} = -308{,}067.5 + 111.52T$	27
	$Q^{Co}_{Al} = -275{,}359 - 73.00T$	28
	$Q^{Co,Al}_{Al} = 60{,}069$	28
	$Q^{Co,Ni}_{Al} = 3371.4$	This work

4.2 Assessment of Atomic Mobility

The thermodynamic description for Ni-Co-Al system was obtained from the previous work of Zhu et al.[27] The calculated isothermal section of the Ni-Co-Al system at 1373 K using the parameters from Ref 27 is presented in Fig. 2(a). The six diffusion couples were also shown in the phase diagram in Fig. 2(b). The atomic mobility parameters for Ni-Al,Co-Al and Ni-Co system were assessed by Zhang et al.,[28] Cui et al.[29] and Campbell et al.,[30] respectively. The atomic mobilities from these literature are listed in Table 3. Based on the existing binary atomic mobilities in Table 3 and the experimental interdiffusion coefficients in Table 2, the atomic mobilities for fcc ternary Ni-Co-Al alloys were assessed in the PARROT module of the DICTRA software.[31] The finally obtained atomic mobility parameters for fcc Ni-Co-Al alloys are listed in Table 3 too.

The calculated main interdiffusion coefficients (numbers in brackets) were compared with the presently experimental ones, as presented in Fig. 3. As can be seen, the calculated main interdiffusivities agree well with the experimental data. Figure 4 presents the comparison between the presently calculated main diffusion coefficients and the experimental values. The calculated logarithmic values of interdiffusion coefficients are equal to the experimental ones along the diagonal line, while the dashed lines refer to the diffusion coefficients with a factor of 2 or 0.5 from the model-predicted main diffusion coefficients in this work. Such a factor is a generally accepted experimental error for measurement of diffusivities. It can be learned from Fig. 4 that the calculated results were in good agreement with the experimental ones.

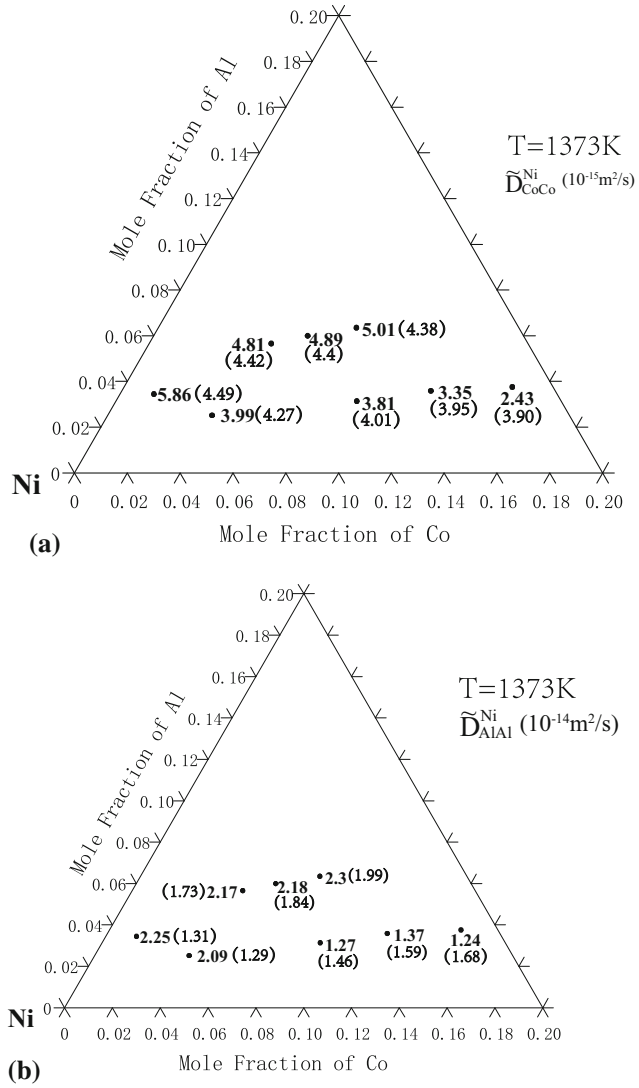

Fig. 3 The calculated main interdiffusion coefficients (numbers in brackets) compared with the experimental measurements. (a) $\tilde{D}^{Ni}_{CoCo}$, (b) $\tilde{D}^{Ni}_{AlAl}$

4.3 Validation of the Present Atomic Mobility

In order to evaluate the reliability of the present mobility database, it is essential to compare the calculated and the observed diffusion behaviors, such as the concentration profiles and diffusion paths. In conjunction with thermodynamics information, the atomic mobilities obtained in the present work were used to calculate the concentration profiles of ternary diffusion couples, as shown in Fig. 5-10. Figure 5 shows the comparison between the calculated concentration profiles of the Ni/Ni-10.7Al-10.4Co (at.%) diffusion couple and the corresponding experimental ones measured in the present work. We can see Al diffuses faster than Co, which is due to the larger diffusion coefficient of Al in fcc Ni-Co-Al solution. As shown in these figures, the calculated results agree well with the experimental values. We can see some inhomogeneity at the terminal end, it is due to the EPMA instability.

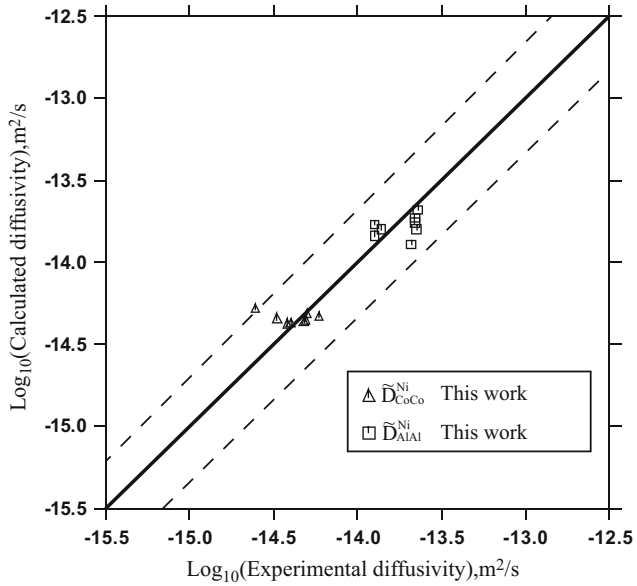

Fig. 4 Comparison between the calculated main interdiffusion coefficients of the fcc Ni-Co-Al system at 1373 K and the experimental values. Dashed lines refer to the diffusion coefficients with a factor of 2 or 0.5 from the model-predicted ones

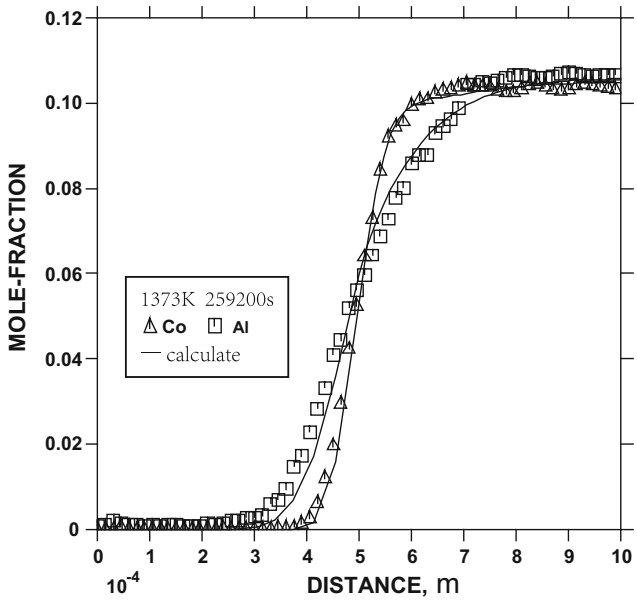

Fig. 5 Comparison between the calculated and the measured concentration profiles for the Ni/Ni-10.7Al-10.4Co (at.%) diffusion couple annealed at 1373 K for 259,200 s

Figure 11 presents the comparison between the calculated and the measured diffusion paths for the six diffusion couples (A1, A2, B1, B2, B3 and B4) annealed at 1373 K for 259,200 s. The S-shaped diffusion paths are observed, which is caused by the difference in diffusion coefficients and the mass balance of the diffusion species in solid-solid diffusion couples.[32] Also, the calculated results agree well with the experimental values.

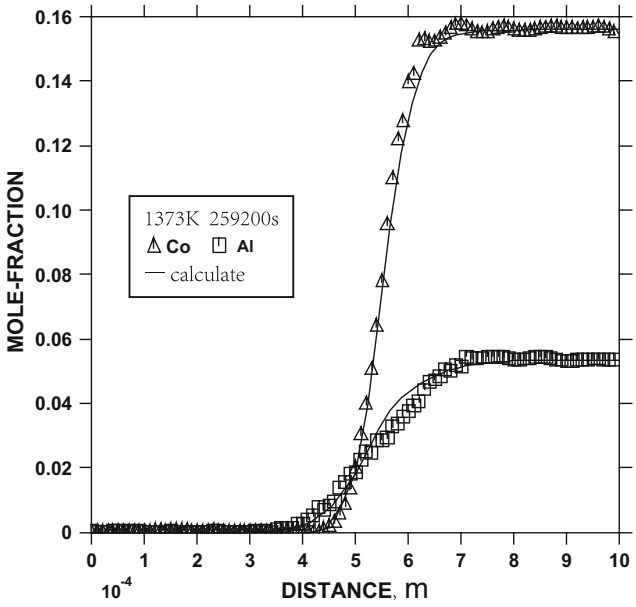

Fig. 6 Comparison between the calculated and the measured concentration profiles for the Ni/Ni-5.4Al-15.5Co (at.%) diffusion couple annealed at 1373 K for 259,200 s

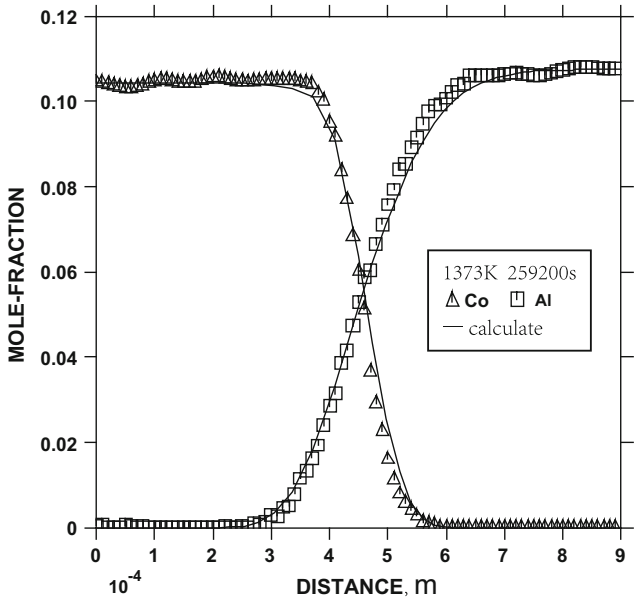

Fig. 8 Comparison between the calculated and the measured concentration profiles for the Ni-Ni10.5Al/Ni-10.5Co (at.%) diffusion couple annealed at 1373 K for 259,200 s

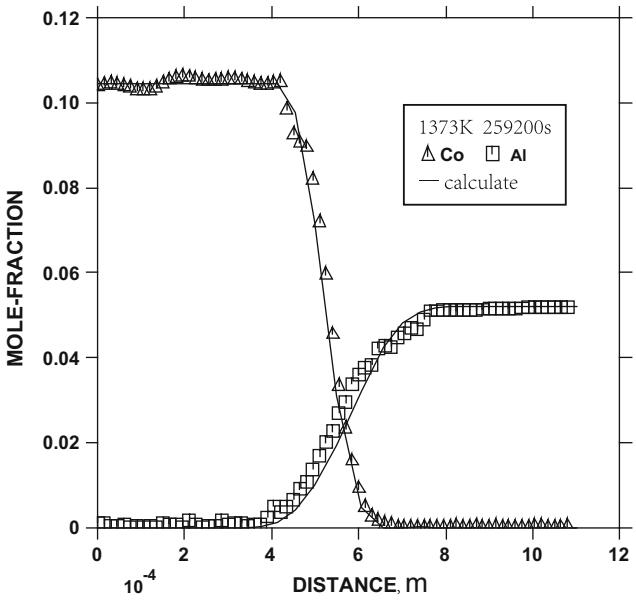

Fig. 7 Comparison between the calculated and the measured concentration profiles for the Ni-5.2Al/Ni-10.5Co (at.%) diffusion couple annealed at 1373 K for 259,200 s

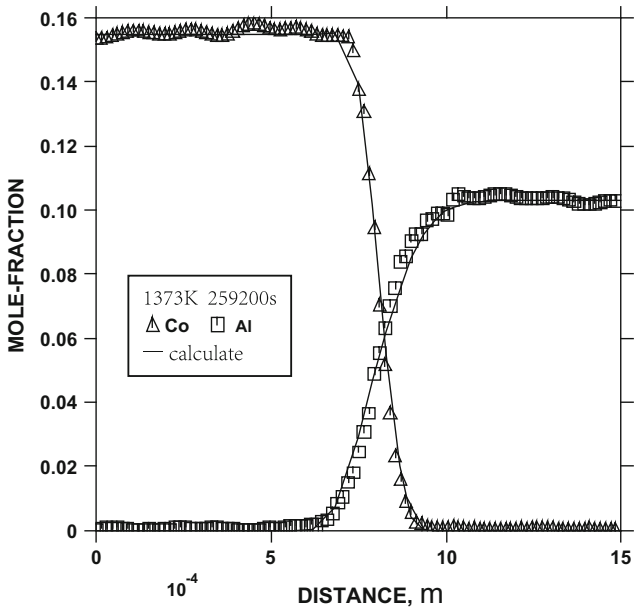

Fig. 9 Comparison between the calculated and the measured concentration profiles for the Ni-10.5Al/Ni-15.5Co (at.%) diffusion couple annealed at 1373 K for 259,200 s

5. Summary

(1) In the present work, a series of ternary solid-solid diffusion couples were prepared. Using Whittle and Green method together with EPMA, the interdiffusion coefficients in fcc Ni-Co-Al alloys at 1373 K were obtained. The reliability of the interdiffusion coefficients was validated by the thermodynamic constraints.

(2) Based on the experimental diffusivities as well as the available thermodynamic description, using the DICTRA software package, atomic mobilities in

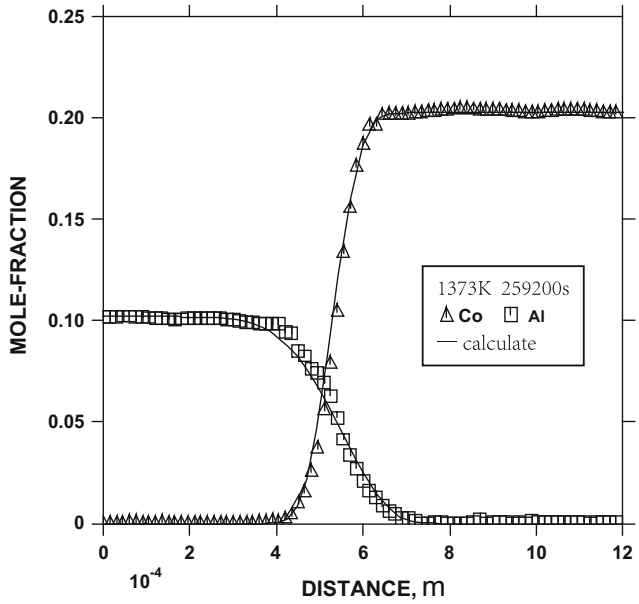

Fig. 10 Comparison between the calculated and the measured concentration profiles for the Ni-10.2Al/Ni-20.3Co (at.%) diffusion couple annealed at 1373 K for 259,200 s

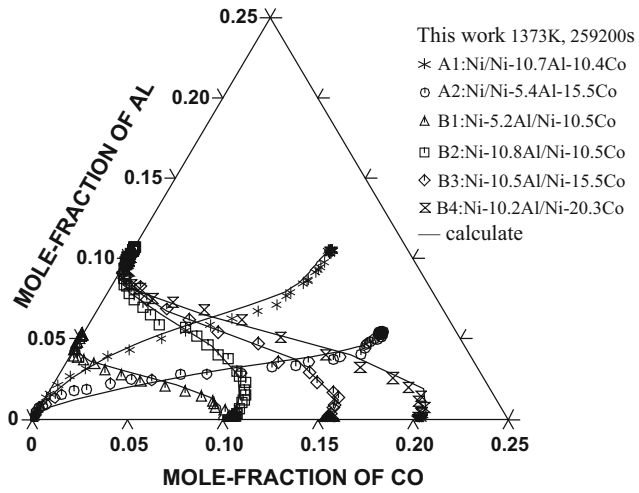

Fig. 11 Comparison between the calculated and the measured diffusion paths for the six diffusion couples (A1, A2, B1, B2, B3 and B4) annealed at 1373 K for 259,200 s

fcc Ni-Co-Al alloys were assessed. The calculated interdiffusivities agree well with the experimental ones.

(3) The assessed atomic mobilities were further validated by the evaluation of concentration profiles and diffusion paths in prepared diffusion couples. The good agreement between the calculations and the experiment data indicates that the presently obtained atomic mobilities are reliable. Furthermore, it can be acted as a supplement of nickel based superalloys diffusion database.

Acknowledgment

This work thanks the support from the Industry-university research project of Aviation Industry Corporation of China (No. CXY2014XD27), the Fundamental Research Funds for the Central Universities (No. 20720140511), Ministry of Science and Technology of China (Grant No. 2014DFA53040) and the National Natural Science Foundation of China (No. 51201145, and No. 51301146).

References

1. R.C. Reed, *The Superalloys: Fundamentals and Applications*, Cambridge University Press, Cambridge, 2006
2. C.T. Sims, N.S. Stoloff, and W.C. Hagel, *Superalloys II*, Wiley, New York, 1987
3. T.M. Pollock and S. Tin, Nickel-Based Superalloys for Advanced Turbine Engines: Chemistry, Microstructure and Properties, *J. Propul. Power*, 2006, **22**, p 361-374
4. S. Walston, A. Cetel, R. MacKay, K. O'hara, D. Duhl, and R. Dreshfield, Joint Development of a Fourth Generation Single Crystal Superalloy, *Superalloys*, 2004, **2004**, p 15-24
5. M.V. Nathal and L.J. Ebert, The Influence of Cobalt, Tantalum, and Tungsten on the Microstructure of Single Crystal Nickel-Base Superalloys, *Metall. Trans. A*, 1985, **16**, p 1849-1862
6. E. Mabruri, S. Sakurai, Y. Murata, T. Koyama, and M. Morinaga, Interdiffusion in Ni-Co-Re and Ni-Co-Ru Systems, *Mater. Trans.*, 2007, **48**, p 2718-2723
7. X.J. Liu, J.Y. Lin, Y. Lu, Y.H. Guo, and C.P. Wang, Assessment of the Atomic Mobility for the fcc Phase of Ni-Co-X (X = Re and Ru) System, *Calphad*, 2014, **45**, p 138-144
8. J. Chen, Y. Liu, G. Sheng, F. Lei, and Z. Kang, Atomic Mobilities, Interdiffusivities and Their Related Diffusional Behaviors in fcc Co-Cr-Ni Alloys, *J. Alloy. Compd.*, 2014, **621**, p 428-433
9. K. Cheng, D. Liu, L. Zhang, Y. Du, S. Liu, and C. Tang, Interdiffusion and Atomic Mobility Studies in Ni-rich fcc Ni-Al-Mn Alloys, *J. Alloy. Compd.*, 2013, **579**, p 124-131
10. M. Hattori, N. Goto, Y. Murata, T. Koyama, and M. Morinaga, Diffusion of Refractory Elements in Ni-Al-X (X: Re, W) Ternary Alloys, *Mater. Trans.*, 2005, **46**, p 163-166
11. E. Mabruri, M. Hattori, K. Hasuike, T. Kunieda, Y. Murata, and M. Morinaga, Al and Re Interdiffusion in the γ-Phase of Ni-Al-Re System, *Mater. Trans.*, 2006, **47**, p 1408-1411
12. J.O. Andersson, T. Helander, L. Höglund, P. Shi, and B. Sundman, Thermo-Calc & DICTRA, Computational Tools for Materials Science, *Calphad*, 2002, **26**, p 273-312
13. A. Borgenstam, L. Höglund, J. Ågren, and A. Engström, DICTRA, a Tool for Simulation of Diffusional Transformations in Alloys, *JPE*, 2000, **21**, p 269-280
14. J. Kirkaldy, Diffusion in Multicomponent Metallic Systems, *Can. J. Phys.*, 1957, **35**, p 435-440
15. J. Morral, Chemical Diffusivities and Their Hidden Concentration Units, *Journal of Phase Equilibria and Diffusion*, 2014, **35**, p 581-586
16. D. Whittle and A. Green, The Measurement of Diffusion Coefficients in Ternary Systems, *Scr. Metall.*, 1974, **8**, p 883-884

17. J. Ågren, Numerical Treatment of Diffusional Reactions in Multicomponent Alloys, *J. Phys. Chem. Solids*, 1982, **43**, p 385-391
18. J. Ågren, Diffusion in Phases with Several Components and Sublattices, *J. Phys. Chem. Solids*, 1982, **43**, p 421-430
19. J. Andersson, L. Höglund, B. Jönsson, J. Ågren, and G. Purdy, *Fundamentals and Applications of Ternary Diffusion*, Pergamon Press, New York, 1990, p 153-163
20. J.O. Andersson and J. Agren, Models for Numerical Treatment of Multicomponent Diffusion in Simple Phases, *J. Appl. Phys.*, 1992, **72**, p 1350-1355
21. B. Jönsson, Ferromagnetic Ordering and Diffusion of Carbon and Nitrogen in bcc Cr-Fe-Ni Alloys, *Zeitschrift für Metallkunde*, 1994, **85**, p 498-501
22. B. Jönsson, Assessment of the Mobility of Carbon in fcc C-Cr-Fe-Ni Alloys, *Zeitschrift für Metallkunde*, 1994, **85**, p 502-509
23. B. Jönsson, On Ferromagnetic Ordering and Lattice Diffusion: A Simple Model, *Zeitschrift für Metallkunde*, 1992, **83**, p 349-355
24. O. Redlich and A. Kister, Algebraic Representation of Thermodynamic Properties and the Classification of Solutions, *Ind. Eng. Chem.*, 1948, **40**, p 345-348
25. M. Hillert, Empirical Methods of Predicting and Representing Thermodynamic Properties of Ternary Solution Phases, *Calphad*, 1980, **4**, p 1-12
26. J. Kirkaldy, D. Weichert, and Z.U. Haq, Diffusion in Multicomponent Metallic Systems: VI. Some Thermodynamic Properties of the D Matrix and the Corresponding Solutions of the Diffusion Equations, *Can. J. Phys.*, 1963, **41**, p 2166-2173
27. J. Zhu, M. Titus, and T. Pollock, Experimental Investigation and Thermodynamic Modeling of the Co-Rich Region in the Co-Al-Ni-W Quaternary System, *J. Phase Equilib. Diffus.*, 2014, **35**, p 595-611
28. L. Zhang, Y. Du, Q. Chen, I. Steinbach, and B. Huang, Atomic Mobilities and Diffusivities in the fcc, L12 and B2 Phases of the Ni-Al System, *Int. J. Mater. Res.*, 2010, **101**, p 1461-1475
29. Y.-W. Cui, B. Tang, R. Kato, R. Kainuma, and K. Ishida, Interdiffusion and atomic mobility for face-centered-cubic Co-Al alloys, *Metall. Mater. Trans. A*, 2011, **42**, p 2542-2546
30. C.E. Campbell, W.J. Boettinger, and U.R. Kattner, Development of a Diffusion Mobility Database for Ni-Base Superalloys, *Acta Mater.*, 2002, **50**, p 775-792
31. B. Jansson, Evaluation of parameters in thermochemical models using different types of experimental data simultaneously (PARROT), Stockholm Materials Research Center: TRITA-MAC-0234, (1984)
32. Y.H. Sohn and M.A. Dayananda, A Double-Serpentine Diffusion Path for a Ternary Diffusion Couple, *Acta Mater.*, 2000, **48**, p 1427-1433